Geosci. Model Dev. Discuss., 5, 1263–1293, 2012
www.geosci-model-dev-discuss.net/5/1263/2012/
doi:10.5194/gmdd-5-1263-2012

Geoscientific Model Development Discussions

Development of a parameterization of black carbon aging for use in general circulation models

N. Oshima[1] **and M. Koike**[2]

[1]Meteorological Research Institute, Tsukuba, Japan
[2]Department of Earth and Planetary Science, Graduate School of Science, University of Tokyo, Tokyo, Japan

Received: 27 April 2012 – Accepted: 2 May 2012 – Published: 16 May 2012

Correspondence to: N. Oshima (oshima@mri-jma.go.jp)

Published by Copernicus Publications on behalf of the European Geosciences Union.

Abstract

A parameterization of black carbon (BC) aging in the atmosphere is developed for use in general circulation models (GCMs) that separately treats size distributions of hydrophobic BC and hydrophilic BC using lognormal modes. The rate of BC aging is expressed as the conversion rate from hydrophobic BC to hydrophilic BC modes (i.e., inverse of the e-folding time of the conversion, $1/\tau_{BC}$). In this study, the conversion rates are estimated using results of detailed calculations by a size and mixing state resolved aerosol box model with numerous initial conditions. We introduce a new concept, the hydrophobic-BC-mass-normalized coating rate (V_{BC}), defined as the rate of increase of the mass concentration of condensed materials on hydrophobic BC normalized by the hydrophobic BC mass concentration. Although the conversion rate largely varies depending on the atmospheric conditions and the concentrations of chemical species, we find that the variations of the conversion rate are generally expressed well by a unique function of V_{BC} for given lognormal size distributions of hydrophobic BC. The parameterized conversion rate is expressed as a function of V_{BC}, which enables the representation of diurnal and seasonal variations of the BC aging rate and its spatial differences in polluted and clean air, while other widely used constant conversion rates cannot. Application of our newly developed parameterization to GCMs will provide more reliable estimates of the spatial distribution of BC and its radiative effects at regional and global scales.

1 Introduction

Most atmospheric aerosol components scatter solar radiation; however, black carbon (BC) aerosols efficiently absorb it and lead to heating of the atmosphere. Because of these light-absorbing effects, BC aerosols have been recognized as one of the most important aerosols for climate forcing (e.g., Hansen et al., 1997; Ramanathan et al., 2001; Jacobson, 2001; Menon et al., 2002; Koren et al., 2004; Ramanathan and

GMDD
5, 1263–1293, 2012

Carmichael, 2008). BC particles are emitted into the atmosphere by incomplete combustion of fossil fuels, biofuels, and biomass. Freshly emitted BC particles are generally bare and have little coating materials on their surface and therefore in a hydrophobic state (Weingartner et al., 1997; Sakurai et al., 2003). They gradually become internally mixed with other aerosols through condensation, coagulation, and photochemical oxidation processes in the atmosphere (aging processes). Internal mixing with sufficient water-soluble compounds changes initially hydrophobic BC to hydrophilic BC, which is able to serve as cloud condensation nuclei (CCN) at a given supersaturation (e.g., Yu, 2000; Seinfeld and Pandis, 2006). Therefore, the aging processes of BC increase the wet scavenging efficiency of BC-containing particles and influence the atmospheric lifetime of BC (Stier et al., 2006) through their removal from the atmosphere by precipitation (Oshima et al., 2012). At the same time, internal mixing with non-absorbing compounds enhances the BC absorption efficiency of solar radiation (Bond et al., 2006). Consequently, aging processes of BC particles play an important role for the spatial distributions of BC and its radiative effects.

General circulation models (GCMs) generally represent aerosol size distribution by multiple lognormal modes and treat the aging processes of BC particles as a conversion of BC from hydrophobic to hydrophilic modes with a characteristic time, because of computational constraints:

$$\left(\frac{\partial[\mathrm{BC_{phob}}]}{\partial t}\right) = -\frac{[\mathrm{BC_{phob}}]}{\tau_{\mathrm{BC}}} \tag{1}$$

$$\left(\frac{\partial[\mathrm{BC_{phil}}]}{\partial t}\right) = \frac{[\mathrm{BC_{phob}}]}{\tau_{\mathrm{BC}}} \tag{2}$$

where $[\mathrm{BC_{phob}}]$ and $[\mathrm{BC_{phil}}]$ are the hydrophobic and hydrophilic BC mass concentrations, respectively, and τ_{BC} is the e-folding time of the conversion. A simple approach using constant values of the conversion rate from hydrophobic BC to hydrophilic BC, such as 24 or 36 h, has been widely used in previous GCM studies (Cooke and Wilson,

GMDD
5, 1263–1293, 2012

1996; Cooke et al., 1999, 2002; Lohmann et al., 1999; Koch, 2001; Chung and Seinfeld, 2002), although the conversion rate is considered to vary depending on atmospheric conditions and concentrations of chemical species during the aging process.

Recently, Koch (2001) and Wilson et al. (2001) calculated the variable conversion rates of BC aging depending on the condensation of sulfuric acid (H_2SO_4), produced from gas-phase oxidation of sulfur dioxide (SO_2). Riemer et al. (2004) presented a detailed parameterization of BC aging using results of mesoscale aerosol model simulations that treated condensation and coagulation of several species of aerosols. They showed that the conversion rate is constant during daytime (i.e., τ_{BC} is 2 h above 250 m and 8 h below) and a function of the number concentration of internally mixed particles during nighttime. However, their parameterization is only applicable for a polluted region over land (e.g., Germany). Liu et al. (2011) developed the parameterization of BC aging using a function of hydroxyl (OH) radical concentration, defined as follows:

$$\frac{1}{\tau_{BC}} = \beta \cdot [\mathrm{OH}] + \delta \tag{3}$$

where β (i.e., a fast aging term, such as condensation) and δ (i.e., a slow aging term such as coagulation, assuming an e-folding conversion time of 20 days) are constants with values $4.6 \times 10^{-12}\,\mathrm{cm^3\,molecule^{-1}\,s^{-1}}$ and $5.8 \times 10^{-7}\,\mathrm{s^{-1}}$, respectively, and [OH] is OH radical concentration. However, use of the constant β value in the fast aging term neglects dependencies of BC aging on condensable materials and their precursors (e.g., H_2SO_4 and SO_2, respectively). The conversion rates have been recognized as one of the key uncertainties in estimating the impacts of BC on climate (Cooke et al., 2002; Chung and Seinfeld, 2005). Recent studies pointed out the necessity of an advanced parameterization of BC aging processes applicable to various atmospheric conditions in GCMs in order to improve the quantitative estimation of the climate impacts of BC (Wilson et al., 2001; Riemer et al., 2004; Croft et al., 2005; Liu et al., 2005; Park et al., 2005; Tsyro et al., 2007; Koch et al., 2009; Liu et al., 2011).

This study develops a new parameterization of the BC aging process for use in GCMs that separately treats size distributions of hydrophobic BC and hydrophilic BC using

GMDD
5, 1263–1293, 2012

lognormal modes. In this study, we focus on the condensation process because it is one of the most important BC aging processes under most atmospheric conditions. The new parameterization is expressed as the conversion rate of BC particles from hydrophobic BC to hydrophilic BC modes, using results of detailed calculations by a size and mixing state resolved aerosol box model. Some results of variations of τ_{BC} derived from the calculations and a method for applying our parameterization to GCMs are also described.

2 Methodology

2.1 MADRID-BC

In this study, we use the Model of Aerosol Dynamics, Reaction, Ionization, and Dissolution (MADRID) (Zhang et al., 2004) with resolution of the mixing state of BC (MADRID-BC) (Oshima et al., 2009a). MADRID-BC is a stand-alone size and mixing state resolved aerosol box model that includes the gas-phase chemistry of the Carbon-Bond Mechanism Version IV (CBM-IV) photochemical mechanism (Gery et al., 1989). Photolysis rates of chemical reactions treated in the Community Multiscale Air Quality (CMAQ) model are utilized in MADRID-BC (Byun and Ching, 1999). Heterogeneous reactions on the surface of particles are also included in MADRID-BC (Jacob, 2000; Zhang et al., 2004). MADRID-BC uses a two-dimensional (2-D) aerosol representation in which aerosol mass and number are given for individual particle diameters and BC mass fractions (see Oshima et al., 2009a, Fig. 1). In addition to BC-containing particles, externally mixed BC-free particles are represented separately. Aerosol species treated in MADRID-BC include sulfate (SO_4^{2-}), ammonium (NH_4^+), nitrate (NO_3^-), sodium (Na^+), chloride (Cl^-), aerosol water, BC, and organic matter (OM). MADRID-BC treats mass transfer between gas and particulate phases using a dynamic (kinetic) non-equilibrium approach developed by Meng et al. (1998), and it enables accurate calculations of the time evolution of the entire BC mixing state resulting from condensation/evaporation

GMDD
5, 1263–1293, 2012

processes. Condensation/evaporation involving secondary organic aerosols (SOAs) and their precursors is not included in the dynamic approach in MADRID-BC, although the method presented in this paper can be extended when SOAs and their precursors are included in condensable materials. The BC aging processes due to coagulation and photochemical oxidation are not included in this study, although contributions of coagulation to BC aging may be important under certain circumstances (e.g., over source regions and during nighttime) (Riemer et al., 2010). The effects of coagulation can be included in our parameterization using a similar approach in Eq. (3) as presented in Sect. 4. MADRID-BC treats homogeneous nucleation processes (Zhang et al., 2004); however, they are not used in this study. The dilution of air, dry and wet deposition, and aqueous-phase chemistry in cloud particles are not included in MADRID-BC. Meteorological conditions (e.g., air density, pressure, temperature (T), relative humidity (RH), and cloud/rain information) are kept constant throughout each MADRID-BC calculation.

MADRID-BC calculates the critical supersaturation of particles using the Köhler equation (Seinfeld and Pandis, 2006). BC is treated as an insoluble concentric core for BC-containing particles and other aerosol components are assumed to be soluble materials that condense onto BC-containing and BC-free particles. When the critical supersaturation of BC-containing particles is lower (greater) than a given air supersaturation, these particles are defined as hydrophilic (hydrophobic) BC, namely CCN (non-CCN). By estimating the CCN activity of BC-containing particles for the entire BC mixing state (i.e., each grid cell in the 2-D aerosol representation), MADRID-BC can calculate mass concentrations of hydrophobic BC and hydrophilic BC for an air parcel at a given supersaturation (Oshima et al., 2009b).

2.2 Calculation of conversion rate ($1/\tau_{BC}$)

The conversion rate of BC particles from hydrophobic to hydrophilic states due to condensation was estimated for various atmospheric conditions, from polluted to clean air, using the MADRID-BC model with numerous initial conditions. Because MADRID-BC calculates mass concentrations of condensed materials (e.g., SO_4^{2-} and NO_3^-) onto BC

GMDD
5, 1263–1293, 2012

particles from their precursor gases (e.g., H_2SO_4 and nitrate acid (HNO_3), principally produced from the oxidation of SO_2 and nitrogen oxides (NO_x), respectively), we used several combinations of initial concentrations of SO_2, NO_x, and ammonia (NH_3) for several combinations of initial values of BC mass concentration, T, and RH. Table 1 shows a summary of all the initial parameters used in the MADRID-BC calculations. The calculations were conducted using every hour photolysis rates for equinox at mid-latitudes, although results obtained in this study can be applied irrespective of latitude and season (see Sects. 3 and 5). The size distribution of the bare BC particles was represented by a lognormal distribution, which was divided into 40 size sections ranging from 0.0215 µm to 10 µm in MADRID-BC. Mass median diameters (D_m) and geometric standard deviations (σ) of the bare BC particles were chosen within ranges of those observed in the atmosphere (Table 2) (Kondo et al., 2006; Moteki et al., 2007; Schwarz et al., 2008a,b). An air supersaturation of 0.1 % was chosen for the definition of hydrophobic BC and hydrophilic BC, because this value is a typical value under ambient conditions reported in the literature (Seinfeld and Pandis, 2006). The dependence of the conversion rate on the definitions of hydrophobic BC and hydrophilic BC is presented in Appendix A.

In this study, the conversion rate of BC particles from hydrophobic BC to hydrophilic BC is defined as the inverse of the time required for the hydrophobic BC mass concentration to decay to $1/e$ of its initial value for each calculation (i.e., $1/\tau_{BC}$) when only condensational growth takes place. We also define that hydrophobic BC particles are initially bare, and therefore τ_{BC} is considered to be the characteristic time required for freshly emitted BC particles to become CCN active. Based on this definition, we calculated the time evolutions of increasing coating amounts on bare BC particles due to condensation for each size bin in MADRID-BC. Considering the typical time steps of instantaneous conversion rates used in GCMs, the MADRID-BC calculations were conducted for the first hour for each initial condition, and increase rates of coating amounts on BC particles (i.e., mass concentration per hour) were estimated for each size bin. By extrapolating the increase rates of coating amounts linearly for all size bins,

GMDD
5, 1263–1293, 2012

we calculated the time evolution of coating amounts on the particles and estimated the time duration (i.e., τ_{BC}) when the hydrophobic BC mass concentration decayed to $1/e$ of its initial value. These calculations were conducted for the individual initial conditions listed in Tables 1 and 2 with the individual hourly photolysis rates. A total of 48 000 calculations were conducted for a given BC size distribution (see Table 1).

3 Parameterization of BC aging

3.1 Hydrophobic-BC-mass-normalized coating rate (V_{BC})

In this study we introduce a new concept, the hydrophobic-BC-mass-normalized coating rate, V_{BC} (h^{-1}), defined as follows:

$$V_{BC} = \frac{1}{[BC_{phob}]} \frac{\partial [M_{BCphob}]}{\partial t} \tag{4}$$

where $\partial[M_{BCphob}]/\partial t$ is the increase rate of the total mass concentration of condensed materials onto initially hydrophobic BC particles per hour. Although the τ_{BC} value largely varies depending on the atmospheric conditions and the concentrations of chemical species, we find that the variation of τ_{BC} is generally captured well by a unique function of V_{BC} for a given lognormal size distribution of BC particles. Fig. 1 shows the variation of τ_{BC} as a function of V_{BC} for all combinations of the initial parameters shown in Table 1 for each given lognormal BC size distribution shown in Table 2 (gray circles). Note that each data point (i.e., each gray circle) shown in Fig. 1 corresponds to a result from the calculation for each initial condition. For example, Fig. 1g shows the results for a lognormal BC size distribution with a D_m of 175 nm and σ of 1.5, which is almost identical to that observed in outflow from anthropogenic sources in Japan (Moteki et al., 2007; Oshima et al., 2009a). Fitting the results shown in Fig. 1g,

GMDD
5, 1263–1293, 2012

we obtain the following relationship between τ_{BC} and V_{BC} (black curve):

$$\tau_{BC} = \frac{a}{V_{BC}} \tag{5}$$

where $a = 0.3746 \pm 0.0004$. This relationship is intuitive; namely, when a large amount of condensable materials is produced for a certain amount of hydrophobic BC particles, the BC particles are quickly coated with condensed species (i.e., greater V_{BC}), and the time required for the conversion from hydrophobic BC to hydrophilic BC becomes shorter (i.e., smaller τ_{BC}). It is noted that V_{BC} is expressed by the total mass concentration of hydrophobic BC and that of condensed amounts on the BC particles, although the τ_{BC} values shown in Fig. 1g are derived from the calculations of increase rates of coating amounts on the BC particles for each size bin.

The relationship between τ_{BC} and V_{BC} in Eq. (5) indicates that when the total condensed amount on hydrophobic BC particles is given for a given size distribution of BC particles, τ_{BC} can be uniquely derived as long as the given BC size distribution is the same. Although variations of τ_{BC} can primarily be represented by V_{BC}, τ_{BC} can also change depending on various factors, such as the chemical composition of coating materials. The spread in τ_{BC} for individual V_{BC} values, shown in Fig. 1g, reflects the differences in the chemical compositions of coating materials through changes in the atmospheric conditions, which affect the critical supersaturation of particles through the solute effect in Köhler theory.

3.2 Dependence on size distribution of BC

Oshima et al. (2009b) showed that the mass fraction of hydrophilic BC particles with respect to total BC particles depends on the size distribution of initially hydrophobic BC particles when the BC particles experience aging processes. In this section we describe the dependence of τ_{BC} on the shape of the lognormal BC size distribution for ranges of D_m of 100–200 nm and σ of 1.5–1.8 (Table 2). We estimated τ_{BC} for these lognormal BC size distributions (Fig. 1) using the same procedure described in

GMDD
5, 1263–1293, 2012

the previous sections. Using the same approach for the Fig. 1g case (Sect. 3.1), we obtain the following relationship between τ_{BC} and V_{BC} for any given lognormal BC size distribution (black curves in Fig. 1):

$$\tau_{BC} = \frac{A(D_m, \sigma)}{V_{BC}} \tag{6}$$

where $A(D_m, \sigma)$ is a constant value representing the dependence on the lognormal BC size distribution. The values of $A(D_m, \sigma)$ for D_m of 100–200 nm and σ of 1.5–1.8 are summarized in Table 2.

According to Eq. (6) and Table 2, the lognormal BC size distribution with the smaller $A(D_m, \sigma)$ value has the smaller conversion time from hydrophobic BC to hydrophilic BC (i.e., faster BC aging). The $A(D_m, \sigma)$ value decreases with the increase in D_m when the $A(D_m, \sigma)$ values with the same σ are compared (Table 2), because the greater D_m shifts the entire BC size distribution to the larger diameter range, and particles with larger diameters generally tend to have a hydrophilic nature (i.e., CCN activity) according to Köhler theory. When the $A(D_m, \sigma)$ values with the same D_m values are compared, the $A(D_m, 1.8)$ values are greater than the $A(D_m, 1.5)$ values, because the greater σ value generally distributes BC particles over a wider size range, increasing the number of BC particles with smaller diameters over the left-hand side of the lognormal distribution (i.e., range with diameters smaller than D_m). Because τ_{BC} is defined as the time required for the hydrophobic BC mass concentration to decay to $1/e$ of its initial value in our calculations and particles with greater diameters generally preferentially become CCN active, the shape of the left-hand side of the lognormal BC distribution is important for τ_{BC} at least within a range of D_m of 100–200 nm. Large variations in the $A(D_m, \sigma)$ values, shown in Table 2, indicate the importance of the size distribution of BC for the BC aging rate.

GMDD
5, 1263–1293, 2012

3.3 Formula for the parameterization

Finally, the formula for the parameterized conversion rate from hydrophobic BC to hydrophilic BC due to condensation is represented as follows:

$$\frac{1}{\tau_{BC}} = \frac{V_{BC}}{A(D_m, \sigma)} \tag{7}$$

where V_{BC} (h^{-1}) is the hydrophobic-BC-mass-normalized coating rate (given by Eq. 4) and $A(D_m, \sigma)$ is a constant value representing the dependence on the lognormal BC size distribution (shown in Table 2). Because the conversion rate in Eq. (7) is expressed as a function of V_{BC}, which depends on the condensed amount onto the hydrophobic BC particles, the newly developed parameterization can represent large variations of the BC aging rate. Therefore, our parameterization of the conversion rate is a more accurate representation than the constant conversion rates widely used in previous studies. Our parameterization is simple and computationally efficient, allowing its application in GCMs.

It is noted that although we assume BC particles are only hydrophobic in this study, our parameterization is still applicable to BC particles internally mixed with water-insoluble particulate organic matter (POM), by replacing the hydrophobic BC mode with a hydrophobic BC/POM mixture mode in models. In addition, even though our parameterization is derived based on condensation of inorganic species, the relationship in Eq. (7) is applicable to particles including SOAs if water-soluble organic and inorganic species play a similar role in the Köhler equation. Our parameterization is also applicable to models that have several aerosol modes other than hydrophobic BC and hydrophilic BC modes, because the conversion rate is derived according to the condensed amounts onto the hydrophobic BC mode. The presence of other aerosol modes changes the condensed amounts onto the hydrophobic BC mode (i.e., V_{BC}) but does not affect the formula in Eq. (7). It is also noted that although we conducted the MADRID-BC calculations for the first hour for each initial condition (Sect. 2), additional

GMDD
5, 1263–1293, 2012

MADRID-BC calculations with different time durations (e.g., one minute) give the same relationship shown in Eq. (7), supporting the validity of Eq. (7) for use in GCMs with any time steps.

4 Application of parameterization to GCMs

In this section, we describe an application method of our parameterization to GCMs, as illustrated in Fig. 2. Our parameterization is applicable to models that separately treats size distributions of hydrophobic BC and hydrophilic BC using lognormal modes.

Step 1. The $A(D_m, \sigma)$ value is taken from Table 2, based on the size distribution of the hydrophobic BC mode represented in the user's GCM.

Step 2. To derive the V_{BC} value by Eq. (4) at each time step in the GCM, the user needs to derive condensed amounts distributed over the hydrophobic BC mode (i.e., $\partial[M_{BCphob}]/\partial t$). If the model explicitly calculates the condensed amounts onto the hydrophobic BC mode, the user can directly derive $\partial[M_{BCphob}]/\partial t$. If the model does not calculate the condensed amounts, the user may use the following weighting factors, W_i, for each aerosol mode i (Pandis et al., 1993; Capaldo et al., 2000):

$$W_i = \frac{N_i D_{p,i}}{\frac{2\lambda_m}{\alpha_i D_{p,i}} + 1} \tag{8}$$

where N_i is the number concentration of particles in mode i, $D_{p,i}$ is the mode diameter of the particles in mode i, λ_m is the air mean free path, and α_i is the accommodation coefficient in mode i on the atmospheric aerosol. These weighting factors are normalized and then used to partition condensable materials, which are produced at each time step, among the aerosol modes, and thus $\partial[M_{BCphob}]/\partial t$ is derived.

Step 3. The conversion rate, $1/\tau_{BC}$, is calculated using Eq. (7) at each time step in the GCM.

GMDD
5, 1263–1293, 2012

Step 4. Finally, a portion of the BC particles in the hydrophobic BC mode is converted to the hydrophilic BC mode using Eqs. (1) and (2). Note that the derived condensed amounts onto the hydrophobic BC mode (i.e., $[M_{\mathrm{BCphob}}]$) have to move to the hydrophilic BC mode (or other internally mixed modes) together with the conversion of the hydrophobic BC particles, because the array of the hydrophobic BC mode may not be allowed to have the condensed amounts (i.e., coatings) in the model.

We describe here several limitations of our parameterization. First, coagulation is not taken into account (Eq. 7). Coagulation may play an important role for BC aging, especially over source regions and during nighttime; therefore application of Eq. (7) may give smaller BC aging rates under those conditions in GCMs. Assuming 80 % hydrophobic and 20 % hydrophilic for initially emitted BC in models, widely used in previous studies (e.g., Cooke et al., 2002; Chung and Seinfeld, 2005), may implicitly include effects of coagulation on BC aging over source regions, because the effects of coagulation are large under conditions with very high aerosol number concentrations. Another approach to include the coagulation effects in our parameterization is adding a coagulation term to Eq. (7). For example, using the slow aging term (i.e., δ) in Eq. (3) following Liu et al. (2011), the parameterization of BC aging including both condensation and coagulation effects is represented by the following equation:

$$\frac{1}{\tau_{\mathrm{BC}}} = \frac{V_{\mathrm{BC}}}{A(D_{\mathrm{m}}, \sigma)} + \delta \tag{9}$$

Second, our parameterization cannot represent evaporation effects of aerosols, because the conversion rate always has positive values. Finally, large uncertainties in calculating production rates of the condensed materials, such as SOAs, in models can lead to errors in the estimation of the conversion rates.

Our newly developed parameterization (i.e., Eq. 9) has been implemented into a global three-dimensional aerosol transport-radiation model, the Spectral Radiation-Transport Model for Aerosol Species (SPRINTARS) (Takemura et al., 2005; Goto et al., 2011a,b) driven by a GCM. The usefulness of our parameterization and impacts of the

GMDD
5, 1263–1293, 2012

BC aging processes on the spatial distribution of BC and aerosol radiative forcing using the SPRINTARS model will be presented in a subsequent paper (Goto et al., Impact of aging process of black carbon aerosol on its spatial distribution, hygroscopicity, and aerosol radiative forcing in a global model, to be submitted to Atmos. Chem. Phys., 2012).

5 Variations of τ_{BC} and V_{BC}

Our parameterization can represent diurnal and seasonal variations of the BC aging rate (i.e., conversion rate, $1/\tau_{BC}$) and its spatial variations through changes in the V_{BC} values. Some examples of these variations of τ_{BC} and the corresponding V_{BC} values for several initial conditions shown in Table 1 are presented for the lognormal BC size distribution with a D_m of 175 nm and σ of 1.5 in this section.

Figure 3a, b show temporal variations of τ_{BC} as a function of the initial SO_2 concentration for a given initial BC, NO_x, and NH_3 concentrations for a T of 298 K and RH of 45 % and those of 278 K and 95 %, respectively. A detailed description of the initial conditions of the chemical species is given in the figure caption. Figure 3c, d show the corresponding V_{BC} values for each τ_{BC} value shown in Fig. 3a, b, respectively. Note that each τ_{BC} value (i.e., colored squares shown in Fig. 3) corresponds to the results of calculations for each initial condition. For the high T and low RH condition (Fig. 3a), BC aging is fast during daytime, with a minimum value of τ_{BC} at noontime (e.g., τ_{BC} is 6.5 h for SO_2 of 5.0 parts per billion by volume (ppbv) at noontime) due to condensation of H_2SO_4, produced from the oxidation of SO_2 by OH radical; however, there is no BC aging during nighttime. This result indicates that τ_{BC} clearly has temporal variations and dependencies on the production of H_2SO_4 directly and OH radical indirectly, as presented by previous studies (e.g., Koch, 2001; Wilson et al., 2001; Riemer et al., 2004; Liu et al., 2011). On the other hand, for the low T and high RH condition (Fig. 3b), BC aging is systematically faster (e.g., τ_{BC} is 2.5 h for SO_2 of 5.0 ppbv at noontime) than the high T and low RH condition (Fig. 3a) during daytime due to condensation of both

GMDD
5, 1263–1293, 2012

H_2SO_4 and HNO_3, produced from the oxidation of nitrogen dioxide (NO_2) by OH radical, and there is relatively slow BC aging during nighttime (e.g., τ_{BC} is about 13 h for any SO_2 concentration) due to condensation of HNO_3, produced from the heterogeneous hydrolysis of dinitrogen pentoxide (N_2O_5), which occurs in aerosol particles. This result indicates that the atmospheric conditions, such as T and RH, are important for τ_{BC} by changing the chemical compositions of condensed materials on BC particles.

In order to examine the dependence of τ_{BC} on RH in detail, variations of τ_{BC} as functions of both the initial SO_2 concentration and RH for the given initial BC, NO_x, and NH_3 concentrations at T of 278 K at noontime and corresponding V_{BC} are shown in Fig. 4a, b, respectively (see the figure caption). Figure 4c, d show mass fractions of SO_4^{2-} and NO_3^- in condensed materials (i.e., coatings) on BC particles, respectively, for each τ_{BC} calculation shown in Fig. 4a. When the lower RH (< 60 %) and the higher RH (> 60 %) conditions are compared, τ_{BC} in the lower RH condition is greater for any given initial SO_2 concentration (Fig. 4a), and the dominant condensed material of BC particles is found to be SO_4^{2-} (about 70 % mass fraction, shown in Fig. 4c). For the higher RH condition, τ_{BC} decreases with the increase in RH, because the NO_3^- amount in condensed materials generally increases with the increase in RH in addition to SO_4^{2-} amount (e.g., a mass fraction of NO_3^- in condensed materials is about 40–50 % for SO_2 of 1.0 ppbv at RH of 75–95 %, shown in Fig. 4d). This result suggests the importance of nitrate aerosols for the aging and the CCN activity of BC particles especially in uplifting air parcels over anthropogenic source regions, because the upward transport of the air parcels is generally associated with high RH conditions.

Figure 5a, b show variations of τ_{BC} and corresponding V_{BC}, respectively, as functions of both the initial SO_2 concentration and BC mass concentration for a given initial NO_x and NH_3 concentrations for T of 298 K and RH of 45 % at noontime (see the figure caption). τ_{BC} depends on the ratio of the SO_2 and BC values, indicating that spatial distributions of emission ratios of precursors of condensable materials to BC (e.g., SO_2/BC ratio) play important roles for the BC aging rate.

GMDD
5, 1263–1293, 2012

It is noted that the inverse relationship between V_{BC} and τ_{BC}, presented in Sect. 3, can also be seen in Figs. 3, 4 and 5. For example, as shown in Fig. 5, τ_{BC} decreases and V_{BC} increases with the increase in the initial SO_2 concentration for any given initial BC mass concentrations, because the greater initial concentration of precursors (i.e., SO_2) produces greater condensable materials (i.e., H_2SO_4) onto the given hydrophobic BC particles (i.e., greater V_{BC}), resulting in a smaller conversion time from hydrophobic BC to hydrophilic BC (i.e., smaller τ_{BC}). It is also noted that V_{BC} can represent several dependencies of τ_{BC} on the atmospheric conditions and the concentrations of chemical species, as shown in Figs. 3, 4 and 5, through changes in the condensed amounts onto hydrophobic BC. The use of V_{BC} enables the representation of the temporal and the spatial variations of the BC aging rate in our parameterization.

6 Summary and conclusions

This study develops a new parameterization of the BC aging process for use in GCMs that separately treats size distributions of hydrophobic BC and hydrophilic BC using lognormal modes. The rate of BC aging is expressed by the conversion rate of BC particles from hydrophobic BC to hydrophilic BC modes (i.e., $1/\tau_{BC}$). We estimate the τ_{BC} values due to condensation process using results from the MADRID-BC model calculations for several combinations of initial concentrations of chemical species and atmospheric conditions (see Table 1) for several given lognormal size distributions of BC particles (see Table 2). In spite of the large variations in the τ_{BC} values depending on the atmospheric conditions and the concentrations of chemical species, we find that the variation of τ_{BC} is generally captured well by a unique function of V_{BC} (the hydrophobic-BC-mass-normalized coating rate, defined by Eq. 4) for any given lognormal size distributions of BC particles for D_m of 100–200 nm and σ of 1.5–1.8 (Table 2). The parameterized conversion rate from hydrophobic BC to hydrophilic BC modes (i.e., $1/\tau_{BC}$) is expressed as a function of V_{BC} with a constant value $A(D_m, \sigma)$ representing the dependence on the lognormal BC size distribution (listed in Table 2) and is presented

GMDD
5, 1263–1293, 2012

in Eqs. (7) and (9). Our newly developed parameterization can represent diurnal (e.g., faster and slower BC aging during daytime and nighttime, respectively) and seasonal (e.g., faster and slower aging in summer and winter, respectively) variations of the BC aging rate and its spatial variations (e.g., over source and remote regions) due to changes in the emission ratios of precursors of condensable materials to BC (e.g., SO_2/BC and NO_x/BC ratios), although other widely used constant conversion rates cannot. Use of our parameterization will provide more reliable estimates of the spatial distribution of BC and its radiative effects in GCMs.

Appendix A

Dependence on definitions of hydrophobic BC and hydrophilic BC

In this study, an air supersaturation of 0.1 % is used for definitions of hydrophobic BC and hydrophilic BC by calculating the CCN activity of particles using the Köhler equation (Sect. 2). Most GCMs generally define hydrophilic BC as particles experiencing water uptake and wet deposition processes as calculated in the model and hydrophobic BC as particles not experiencing these processes. This classification method only provides arrays of hydrophobic BC and hydrophilic BC in models and does not take into account the hydrophobic or hydrophilic natures of BC-containing particles themselves. However, our definition can give the degree of hydrophobic and hydrophilic states for the hydrophobic BC and the hydrophilic BC modes, respectively, in models based on supersaturation. It is noted that supersaturation is initially used for the definition of BC particles in models, and we need not calculate supersaturation itself in models (e.g., models need not calculate supersaturations for aerosol activation).

In this appendix, we describe the dependence of τ_{BC} on the definitions of hydrophobic BC and hydrophilic BC, namely supersaturation, s (%), between 0.05 % and 1 % for all lognormal BC size distributions shown in Table 2. The dependence is expressed by $F(s) \equiv \tau_{BC}(s)/\tau_{BC}(0.1)$, where $\tau_{BC}(s)$ and $\tau_{BC}(0.1)$ are the τ_{BC} values for

GMDD
5, 1263–1293, 2012

a supersaturation of any s % and 0.1 %, respectively. $F(s)$ is approximately derived from Köhler theory as follows:

$$F(s) \equiv \frac{\tau_{BC}(s)}{\tau_{BC}(0.1)} = \left(\frac{\ln\left(1 + \frac{0.1}{100}\right)}{\ln\left(1 + \frac{s}{100}\right)} \right)^2 \tag{A1}$$

Figure A1 shows comparisons of the $F(s)$ values as a function of s calculated by Eq. (A1) (black curves) with the $\tau_{BC}(s)/\tau_{BC}(0.1)$ values derived from the calculation results using all combinations of the initial parameters (shown in Table 1) between 0.05 % and 1 % with a 0.05 % interval (gray circles) for each given lognormal BC size distribution (shown in Table 2). The good agreements shown in Fig. A1 indicate the validity of the use of Eq. (A1) to represent the dependence on the supersaturation, at least between 0.05 % and 1 %, for the given lognormal BC size distributions listed in Table 2.

Taking into account this dependence, a formula for the parameterized conversion rate from hydrophobic BC to hydrophilic BC presented in Eq. (7) is represented as follows:

$$\frac{1}{\tau_{BC}} = \frac{V_{BC}}{A(D_m, \sigma) \cdot F(s)} \tag{A2}$$

where V_{BC} (h^{-1}) is the hydrophobic-BC-mass-normalized coating rate (given by Eq. 4), $A(D_m, \sigma)$ is a constant value representing the dependence on the lognormal BC size distribution (shown in Table 2), and $F(s)$ is a correction factor for the definition of hydrophobic BC and hydrophilic BC (given by Eq. A1).

Finally, an application method of this parameterization (Eq. A2) to GCMs is described here. If the user wants to change the definition of hydrophobic BC and hydrophilic BC in the user's GCM, one value of supersaturation, s %, has to be chosen by the user to calculate $F(s)$ using Eq. (A1). For example, if the user wants to give the degrees of hydrophilic particles as those activated for stratiform clouds, the user can give smaller

GMDD
5, 1263–1293, 2012

values of s, such as 0.05 %, for a correction factor $F(s)$. The subsequent method is described in Sect. 4.

Acknowledgements. This work was supported by the Ministry of Education, Culture, Sports, Science, and Technology and Japan Society for the Promotion of Science (MEXT/JSPS) through the Grant-in-Aid for Young Scientists (B) (KAKENHI) 23710029. This work was supported in part by the MEXT/JSPS Grant-in-Aid for Scientific Research (S) (KAKENHI) 23221001 and the global environment research fund of the Japanese Ministry of the Environment (A-0803 and A-1101). This study was conducted as a part of the Mega-Cities: Asia Task under the framework of the International Global Atmospheric Chemistry (IGAC) project. We thank T. Takemura, D. Goto, and M. Kajino for providing helpful comments on this paper.

References

Bond, T., Habib, G., and Bergstrom, R. W.: Limitations in the enhancement of visible light absorption due to mixing state, J. Geophys. Res., 111, D20211, doi:10.1029/2006JD007315, 2006.

Byun, D. W. and Ching, J. K. S.: Science algorithms of the EPA Models-3 Community Multiscale Air Quality (CMAQ) modeling system, US Environmental Protection Agency, Office of Research and Development, Washington, DC, EPA/600/R-99/030, 1999.

Capaldo, K. P., Pilinis, C., and Pandis, S. N.: A computationally efficient hybrid approach for dynamic gas/aerosol transfer in air quality models, Atmos. Environ., 34, 3617–3627, 2000.

Chung, S. H. and Seinfeld, J. H.: Global distribution and climate forcing of carbonaceous aerosols, J. Geophys. Res., 107, 4407, doi:10.1029/2001JD001397, 2002.

Chung, S. H. and Seinfeld, J. H.: Climate response of direct radiative forcing of anthropogenic black carbon, J. Geophys. Res., 110, D11102, doi:10.1029/2004JD005441, 2005.

Cooke, W. F. and Wilson, J. J. N.: A global black carbon aerosol model, J. Geophys. Res., 101, D14, 19395–19409, 1996.

Cooke, W. F., Liousse, C., Cachier, H., and Feichter, J.: Construction of a 1 × 1 fossil fuel emission data set for carbonaceous aerosol and implementation and radiative impact in the ECHAM4 model, J. Geophys. Res., 104, 22137–22162, 1999.

GMDD
5, 1263–1293, 2012

Cooke, W. F., Ramaswamy, V., and Kasibhatla, P.: A general circulation model study of the global carbonaceous aerosol distribution, J. Geophys. Res., 107, 4279, doi:10.1029/2001JD001274, 2002.

Croft, B., Lohmann, U., and von Salzen, K.: Black carbon ageing in the Canadian Centre for Climate modelling and analysis atmospheric general circulation model, Atmos. Chem. Phys., 5, 1931–1949, doi:10.5194/acp-5-1931-2005, 2005.

Gery, M. W., Whitten, G. Z., Killus, J. P., and Dodge, M. C.: A photochemical kinetics mechanism for urban and regional scale computer modeling, J. Geophys. Res., 94, 12925–12956, 1989.

Goto, D., Nakajima, T., Takemura, T., and Sudo, K.: A study of uncertainties in the sulfate distribution and its radiative forcing associated with sulfur chemistry in a global aerosol model, Atmos. Chem. Phys., 11, 10889–10910, doi:10.5194/acp-11-10889-2011, 2011a.

Goto, D., Schutgens, N. A. J., Nakajima, T., and Takemura T.: Sensitivity of aerosol to assumed optical properties over Asia using a global aerosol model and AERONET, Geophys. Res. Lett., 38, L17810, doi:10.1029/2011GL048675, 2011b.

Hansen, J., Sato, M., and Ruedy, R.: Radiative forcing and climate response, J. Geophys. Res., 102, 6831–6864, 1997.

Jacob, D. J.: Heterogeneous chemistry and tropospheric ozone, Atmos. Environ., 34, 2131–2159, 2000.

Jacobson, M. Z.: Strong radiative heating due to the mixing state of black carbon in atmospheric aerosols, Nature, 409, 695–697, 2001.

Koch, D.: Transport and direct radiative forcing of carbonaceous and sulfate aerosols in the GISS GCM, J. Geophys. Res., 106, 20311–20332, 2001.

Koch, D., Schulz, M., Kinne, S., McNaughton, C., Spackman, J. R., Balkanski, Y., Bauer, S., Berntsen, T., Bond, T. C., Boucher, O., Chin, M., Clarke, A., De Luca, N., Dentener, F., Diehl, T., Dubovik, O., Easter, R., Fahey, D. W., Feichter, J., Fillmore, D., Freitag, S., Ghan, S., Ginoux, P., Gong, S., Horowitz, L., Iversen, T., Kirkevåg, A., Klimont, Z., Kondo, Y., Krol, M., Liu, X., Miller, R., Montanaro, V., Moteki, N., Myhre, G., Penner, J. E., Perlwitz, J., Pitari, G., Reddy, S., Sahu, L., Sakamoto, H., Schuster, G., Schwarz, J. P., Seland, Ø., Stier, P., Takegawa, N., Takemura, T., Textor, C., van Aardenne, J. A., and Zhao, Y.: Evaluation of black carbon estimations in global aerosol models, Atmos. Chem. Phys., 9, 9001–9026, doi:10.5194/acp-9-9001-2009, 2009.

Kondo, Y., Komazaki, Y., Miyazaki, Y., Moteki, N., Takegawa, N., Kodama, D., Deguchi, S., Nogami, M., Fukuda, M., Miyakawa, T., Morino, Y., Koike, M., Sakurai, H., and Ehara, K.:

Temporal variations of elemental carbon in Tokyo, J. Geophys. Res., 111, D12205, doi:10.1029/2005JD006257, 2006.
Koren, I., Kaufman, Y. J., Remer, L. A., and Martins, J. V.: Measurement of the effect of Amazon smoke on inhibition of cloud formation, Science, 303, 1342–1345, 2004.
Liu, J., Fan, S., Horowitz, L. W., and Levy II, H.: Evaluation of factors controlling long-range transport of black carbon to the Arctic, J. Geophys. Res., 116, D04307, doi:10.1029/2010JD015145, 2011.
Liu, X., Penner, J. E., and Herzog, M.: Global modeling of aerosol dynamics: model description, evaluation, and interactions between sulfate and nonsulfate aerosols, J. Geophys. Res., 110, D18206, doi:10.1029/2004JD005674, 2005.
Lohmann, U., Feichter, J., Chuang, C. C., and Penner, J. E.: Predicting the number of cloud droplets in the ECHAM GCM, J. Geophys. Res., 104, 9169–9198, 1999.
Meng, Z., Dabdub, D., and Seinfeld, J. H.: Size-resolved and chemically resolved model of atmospheric aerosol dynamics, J. Geophys. Res., 103, 3419–3435, 1998.
Menon, S., Hansen, J., Nazarenko, L., and Luo, Y.: Climate effects of black carbon aerosols in China and India, Science, 297, 2250–2253, 2002.
Moteki, N., Kondo, Y., Miyazaki, Y., Takegawa, N., Komazaki, Y., Kurata, G., Shirai, T., Blake, D. R., Miyakawa, T., and Koike, M.: Evolution of mixing state of black carbon particles: aircraft measurements over the Western Pacific in March 2004, Geophys. Res. Lett., 34, L11803, doi:10.1029/2006GL028943, 2007.
Oshima, N., Koike, M., Zhang, Y., Kondo, Y., Moteki, N., Takegawa, N., and Miyazaki, Y.: Aging of black carbon in outflow from anthropogenic sources using a mixing state resolved model: 1. model development and evaluation, J. Geophys. Res., 114, D06210, doi:10.1029/2008JD010680, 2009a.
Oshima, N., Koike, M., Zhang, Y., and Kondo, Y.: Aging of black carbon in outflow from anthropogenic sources using a mixing state resolved model: 2. aerosol optical properties and cloud condensation nuclei activities, J. Geophys. Res., 114, D18202, doi:10.1029/2008JD011681, 2009b.
Oshima, N., Kondo, Y., Moteki, N., Takegawa, N., Koike, M., Kita, K., Matsui, H., Kajino, M., Nakamura, H., Jung, J. S., and Kim, Y. J.: Wet removal of black carbon in Asian outflow: Aerosol Radiative Forcing in East Asia (A-FORCE) aircraft campaign, J. Geophys. Res., 117, D03204, doi:10.1029/2011JD016552, 2012.

GMDD
5, 1263–1293, 2012

Pandis, S. N., Wexler, A. S., and Seinfeld, J. H.: Secondary organic aerosol formation and transport – II. Predicting the ambient secondary organic aerosol size distribution, Atmos. Environ., 27, 2403–2416, 1993.

Park, R. J., Jacob, D. J., Palmer, P. I., Clarke, A. D., Weber, R. J., Zondlo, M. A., Eisele, F. L., Bandy, A. R., Thornton, D. C., Sachse, G. W., and Bond, T.: Export efficiency of black carbon aerosol in continental outflow: global implications, J. Geophys. Res., 110, D11205, doi:10.1029/2004JD005432, 2005.

Ramanathan, V. and Carmichael, G.: Global and regional climate changes due to black carbon, Nat. Geosci., 1, 221–227, 2008.

Ramanathan, V., Crutzen, P. J., Kiehl, J. T., and Rosenfeld, D.: Aerosols, climate, and the hydrological cycle, Science, 294, 2119–2124, 2001.

Riemer, N., Vogel, H., and Vogel, B.: Soot aging time scales in polluted regions during day and night, Atmos. Chem. Phys., 4, 1885–1893, doi:10.5194/acp-4-1885-2004, 2004.

Riemer, N., West, M., Zaveri, R. A., and Easter, R. C.: Estimating soot aging time scales with a particle-resolved aerosol model, J. Aerosol Sci., 41, 143–158, 2010.

Sakurai, H., Park, K., McMurry, P. H., Zarling, D. D., Kittelson, D. B., and Ziemann, P. J.: Size-dependent mixing characteristics of volatile and nonvolatile components in diesel exhaust aerosols, Environ. Sci. Technol., 34, 5487–5495, 2003.

Schwarz, J. P., Spackman, J. R., Fahey, D. W., Gao, R. S., Lohmann, U., Stier, P., Watts, L. A., Thomson, D. S., Lack, D. A., Pfister, L., Mahoney, M. J., Baumgardner, D., Wilson, J. C., and Reeves, J. M.: Coatings and their enhancement of black carbon light absorption in the tropical atmosphere, J. Geophys. Res., 113, D03203, doi:10.1029/2007JD009042, 2008a.

Schwarz, J. P., Gao, R. S., Spackman, J. R., Watts, L. A., Thomson, D. S., Fahey, D. W., Ryerson, T. B., Peischl, J., Holloway, J. S., Trainer, M., Frost, G. J., Baynard, T., Lack, D. A., de Gouw, J. A., Warneke, C., and Del Negro, L. A.: Measurement of the mixing state, mass, and optical size of individual black carbon particles in urban and biomass burning emissions, J. Geophys. Res., 35, L13810, doi:10.1029/2008GL033968, 2008b.

Seinfeld, J. H. and Pandis, S. N.: Atmospheric Chemistry and Physics: from Air Pollution to Climate Change, 2nd edn., John Wiley & Sons, New York, USA, 2006.

Stier, P., Seinfeld, J. H., Kinne, S., Feichter, J., and Boucher, O.: Impact of nonabsorbing anthropogenic aerosols on clearsky atmospheric absorption, J. Geophys. Res., 111, D18201, doi:10.1029/2006JD007147, 2006.

GMDD
5, 1263–1293, 2012

Takemura, T., Nozawa, T. T., Emori, S., Nakajima, T. Y., and Nakajima, T.: Simulation of climate response to aerosol direct and indirect effects with aerosol transport-radiation model, J. Geophys. Res., 110, D02202, doi:10.1029/2004JD005029, 2005.

Tsyro, S., Simpson, D., Tarrason, L., Klimont, Z., Kupiainen, K., Pio, C., and Yttri, K. E.: Modeling of elemental carbon over Europe, J. Geophys. Res., 112, D23S19, doi:10.1029/2006JD008164, 2007.

Weingartner, E., Burtscher, H., and Baltensperger, U.: Hygroscopic properties of carbon and diesel soot particles, Atmos. Environ., 31, 2311–2327, 1997.

Wilson, J., Cuvelier, C., and Raes, F.: A modeling study of global mixed aerosol fields, J. Geophys. Res., 106, 34081–34108, 2001.

Yu, S.: Role of organic acids (formic, acetic, pyruvic and oxalic) in the formation of cloud condensation nuclei (CCN): a review, Atmos. Res., 53, 185–217, 2000.

Zhang, Y., Pun, B., Vijayaraghavan, K., Wu, S. Y., Seigneur, C., Pandis, S. N., Jacobson, M. Z., Nenes, A., and Seinfeld, J. H.: Development and application of the model of aerosol dynamics, reaction, ionization, and dissolution (MADRID), J. Geophy. Res., 109, D01202, doi:10.1029/2003JD003501, 2004.

GMDD
5, 1263–1293, 2012

Table 1. Summary of all initial parameters used in the calculations.*

Species	Values
BC, $\mu g\,m^{-3}$	0.1, 0.5, 1.0, 5.0, 10.0
SO_2, ppbv	0.1, 0.5, 1.0, 5.0, 10.0
NO_x, ppbv	0.1, 1.0, 10.0
NH_3, ppbv	0.1, 1.0, 10.0
T, K	278, 298
RH, %	25, 35, 45, 55, 65, 75, 85, 95

* To reduce the number of calculations, we only used combinations of NO_x and NH_3 values (NO_x, NH_3) of (0.1, 0.1), (0.1, 10.0), (1.0, 1.0), (10.0, 0.1), and (10.0, 10.0) with combinations of all the other parameters. A total of 48 000 calculations, namely 5 (BC) × 5 (SO_2) × 5 (NO_x and NH_3) × 2 (T) × 8 (RH) × 24 (hourly photolysis rates), were conducted for a given BC size distribution.

GMDD
5, 1263–1293, 2012

Table 2. Summary of all lognormal size distributions of BC used in the calculations and the corresponding $A(D_m, \sigma)$ values.*

	σ	
D_m, nm	1.5	1.8
100	2.00	2.45
125	1.04	1.28
150	0.583	0.743
175	0.375	0.474
200	0.256	0.316

*D_m is the mass median diameter (in nm) and σ is the geometric standard deviation of a lognormal size distribution of hydrophobic BC particles.

GMDD
5, 1263–1293, 2012

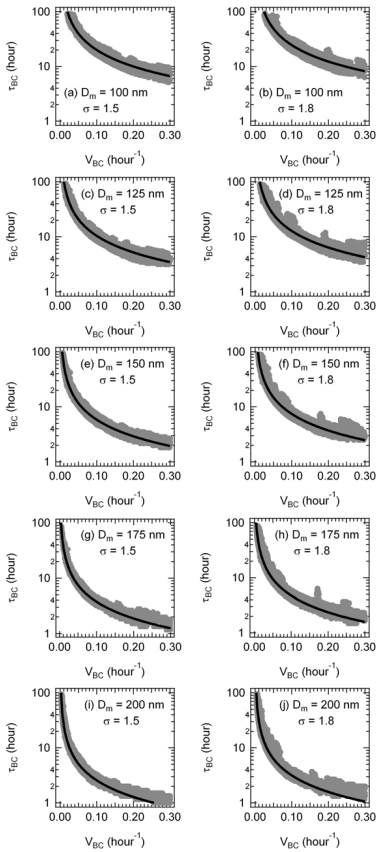

Fig. 1. Relationships between τ_{BC} (e-folding time of the conversion from hydrophobic BC to hydrophilic BC) and V_{BC} (hydrophobic-BC-mass-normalized coating rate, defined by Eq. 4) for all combinations of the initial parameters shown in Table 1 for each given lognormal BC size distribution shown in Table 2 (gray circles). The black curves show the fitted curve expressed by Eq. (6).

GMDD
5, 1263–1293, 2012

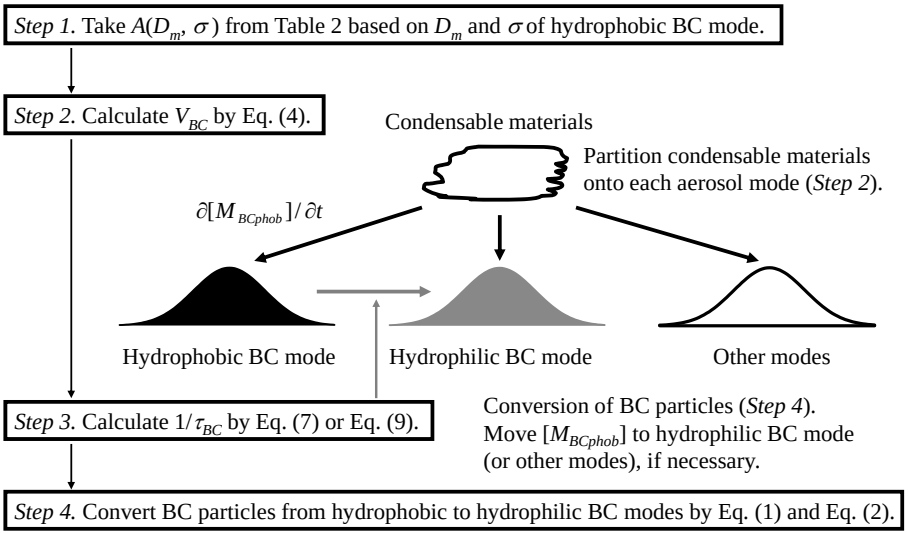

Fig. 2. Schematic diagram of an application method of the parameterization developed in this study to GCMs.

GMDD
5, 1263–1293, 2012

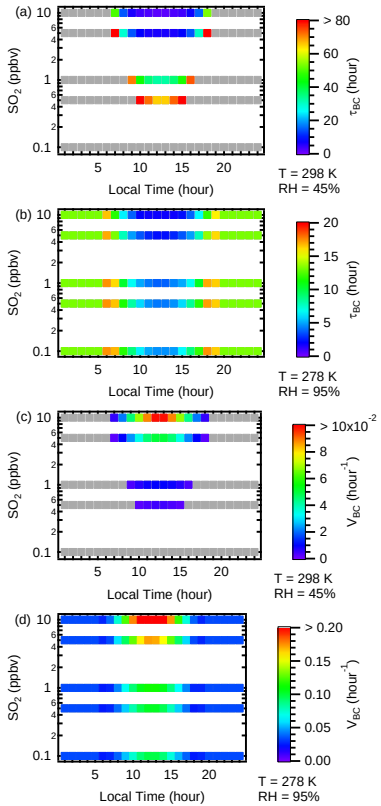

Fig. 3. Temporal variations of **(a)** τ_{BC} and **(c)** corresponding V_{BC} for T of 298 K and RH of 45 % and **(b)** τ_{BC} and **(d)** corresponding V_{BC} for T of 278 K and RH of 95 % as a function of the initial SO_2 concentration for a given initial BC mass concentration of 1.0 $\mu g\,m^{-3}$, NO_x mixing ratio of 1.0 ppbv, and NH_3 mixing ratio of 1.0 ppbv for the lognormal BC size distribution with a D_m of 175 nm and σ of 1.5. Note that τ_{BC} values greater than 120 h are indicated in gray.

GMDD
5, 1263–1293, 2012

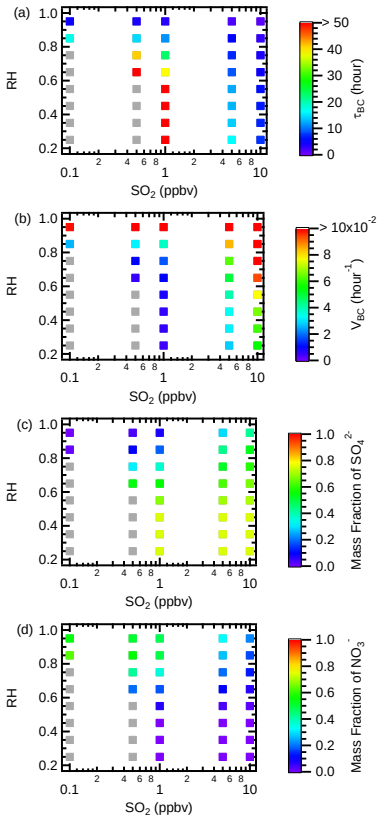

Fig. 4. Variations of **(a)** τ_{BC} and **(b)** correspondingV_{BC} as functions of both the initial SO_2 concentration and RH for a given initial BC mass concentration of 1.0 µg m^{-3}, NO_x mixing ratio of 1.0 ppbv, and NH_3 mixing ratio of 1.0 ppbv for the lognormal BC size distribution with a D_m of 175 nm and σ of 1.5 at T of 278 K at noontime. Mass fractions of **(c)** SO_4^{2-} and **(d)** NO_3^- in condensed materials on BC particles for each τ_{BC} shown in Fig. 4a. Note that τ_{BC} values greater than 120 h are indicated in gray.

GMDD
5, 1263–1293, 2012

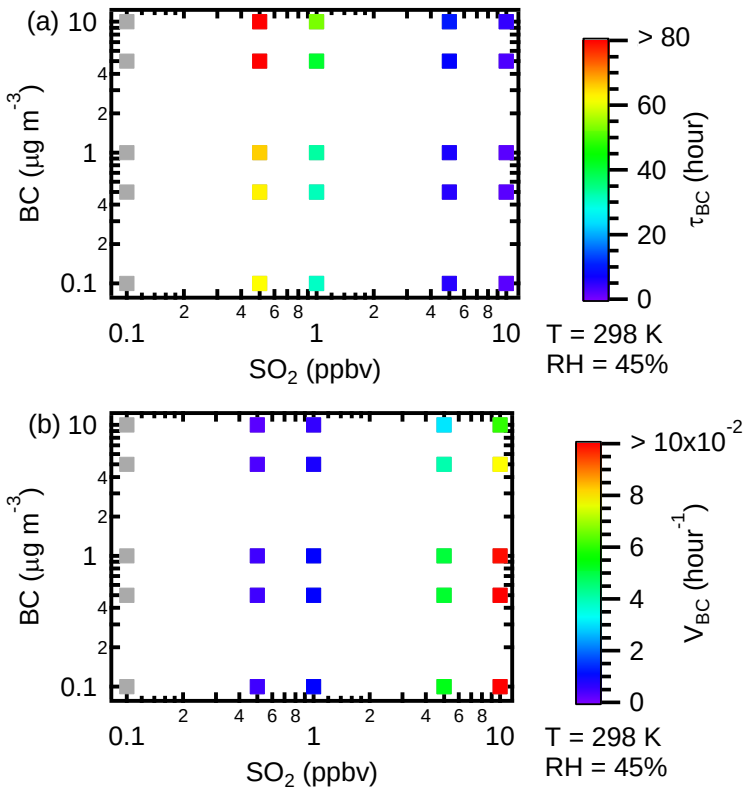

Fig. 5. Variations of **(a)** τ_{BC} and **(b)** corresponding V_{BC} as functions of both the initial SO_2 concentration and BC mass concentration for a given initial NO_x mixing ratio of 1.0 ppbv and NH_3 mixing ratio of 1.0 ppbv for the lognormal BC size distribution with a D_m of 175 nm and σ of 1.5 for T of 298 K and RH of 45 % at noontime. Note that τ_{BC} values greater than 120 h are indicated in gray.

GMDD
5, 1263–1293, 2012

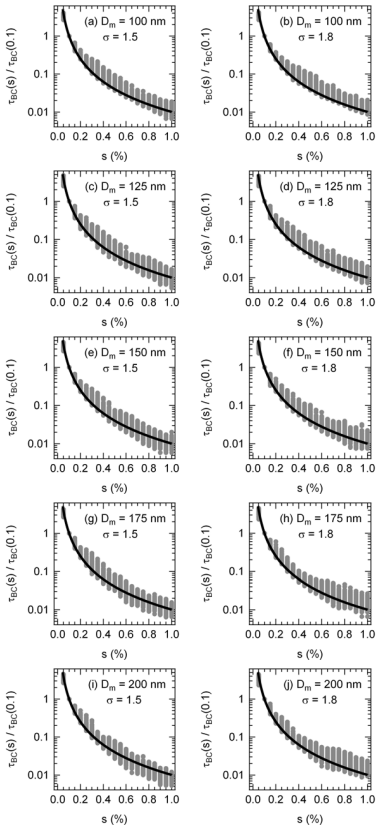

Fig. A1. Comparisons of the $F(s)$ ($\equiv \tau_{BC}(s)/\tau_{BC}(0.1)$) values as a function of s (supersaturation, %) calculated by Eq. (A1) (black curves) with the $\tau_{BC}(s)/\tau_{BC}(0.1)$ values derived from the calculation results using all combinations of the initial parameters shown in Table 1 between 0.05 % and 1 % with a 0.05 % interval (gray circles) for each given lognormal BC size distribution shown in Table 2.

GMDD
5, 1263–1293, 2012